

Spectral Characterization in the Near and Mid-field of Military Jet Aircraft Noise

Tracianne B. Neilsen¹, Kent L. Gee²
Brigham Young University, Provo, UT, 84602

Michael M. James³
Blue Ridge Research and Consulting, LLC, Asheville, NC, 28801

Spatial dependence of levels and spectral characteristics of the near-field noise spectra from the afterburning F-22A Raptor and their transition toward far-field behavior are described. It is shown that the measured spectra in the vicinity of the aircraft show relatively good agreement with overall shape of large and fine-scale similarity spectra, with two exceptions. First, the measured spectral shapes have shallower slopes at high frequencies than the similarity spectra at most downstream locations. The variation in high-frequency slope with downstream distance is quantified and, in the vicinity of the maximum radiation direction, approaches the $1/f^2$ limit associated with shock formation. This measured slope agrees with some previous laboratory and full-scale measurements of supersonic jet noise. Second, the spectra at downstream distances corresponding to the region of maximum radiation exhibit a double peak, a characteristic not predicted by the similarity spectra nor seen in laboratory-scale measurements. In addition, the maximum in the peak-frequency region does not vary continuously with downstream distance, but rather exhibits discrete frequency jumps, with relative contributions of the different peaks varying as a function of downstream distance. These observations have implications in finding ties between the noise from high performance, full-scale engines and laboratory-scale experiments and computational modeling efforts. Furthermore, they indicate the limitations in applying the present similarity spectra models to full-scale engine noise.

Nomenclature

| | |
|-------|---|
| f | = frequency, Hz |
| FSS | = fine-scale structures |
| LSS | = large-scale structures |
| OASPL | = overall sound pressure level, dB re 20 μ Pa |
| OTO | = one-third octave |
| SPL | = one-third octave band pressure level, dB re 20 μ Pa |

¹ Part-Time Assistant Professor, Dept. of Physics and Astronomy, N283 ESC, AIAA Member.

² Associate Professor, Dept. of Physics and Astronomy, N283 ESC, AIAA Senior Member.

³ Senior Principal Engineer, 15 W. Walnut St. Suite C

x = sideline distance, m
 y = vertical distance, m
 z = downstream distance, m

I. Introduction

AN understanding of the spectral characteristics in the near and mid-fields of a supersonic jet is important for investigating personnel exposure issues, noise reduction technology effectiveness, and noise source extent. However, this is made difficult because there is no physics-based model to describe how to extrapolate inward from far-field measurements to recreate the near field of an extended, partially correlated source, nor how to interpolate between coarsely sampled measurement positions. Consequently, detailed noise measurements in the near and mid-fields of the F-22A Raptor¹ can shed insights into the spatial dependence of levels and spectral characteristics. These measurements permit exploration of how these characteristics change with range and provide an important benchmark against the results of near-field, laboratory-scale measurements or computational aeroacoustics calculations. Some of the spectral features that merit consideration are the attribution of measured spectral shapes at different locations to large and fine-scale turbulent structures, the influence of the source spatial extent and radiated directivity of the levels at key frequencies, the effects of geometric spreading and nonlinear propagation as a function of distance.

Although various far-field methods, such as beamforming² and reflector-based directional microphones³⁻⁵ have been employed to extract equivalent source characteristics and improve understanding of large and fine-scale radiation from jets, near-field measurements and processing methods provide more direct insight into source spatial extent and radiation properties. These algorithms include near-field acoustical holography⁶⁻¹⁰ and instability-wave¹¹⁻¹³ and other^{14,15} equivalent source models. Near-field level and spectral surveys of laboratory-scale jet noise fields have included those by Yu and Dosanjh,¹⁶ Baars *et al.*,^{17,18} Gee *et al.*,^{19,20} and Mora *et al.*²¹ Previous near and mid-field measurements on full-scale engines are more limited, but include analyses of noise radiated from both uninstalled²² and installed^{1,23,24} engines. Some studies^{19,25,17,22} described or demonstrated the difficulty in separating the influence of various physical cause(s) on the spectral characteristics at different ranges. The physical causes that determine the spectra include the directionality of jet noise, nonspherical spreading in the near field, a complex measurement environment, air absorption, and nonlinear propagation effects. The intertwined nature of the effects helps motivate the need for additional understanding of spectral characteristics in the near field.

One of the important aspects of supersonic jet noise from high-performance jet engines is nonlinear propagation. Although there have been a number of studies on the nonlinear propagation of noise from laboratory-scale jets,^{19,20,17,25-28} full-scale jet engine measurements demonstrate more clearly the effect of nonlinearity on spectral evolution and its significance. Prior measurements on full-scale jet engines^{22,29,30} have resulted in a better understanding of noise properties in the far field at high engine powers. Furthermore, nonlinear propagation effects, evidenced by shock-wave formation and a high-frequency spectral energy transfer, are more observable in the far field of a high-performance aircraft. For example, Gee *et al.*²⁹ found good agreement between nonlinearly modeled and measured F-22A spectra at 305 m over a 55° measurement aperture to the side and aft of the aircraft, even for an intermediate engine condition. Replication of the equivalent spectral bandwidths and scaled far-field ranges of such a full-scale experiment is currently impossible in a laboratory setting. However, with a better

understanding of near-field processes in full-scale jets, laboratory-scale experiments can be better designed to mimic the full-scale conditions and the corresponding radiated fields and to extract important physical insights.

The principal goal of the present paper is to better characterize the properties of the near-field noise spectra from the afterburning F-22A Raptor¹ and their transition toward far-field behavior. This paper is a continuation of previous analyses^{31,32} that compared full-scale, supersonic jet noise spectra against the Tam *et al.*^{33,34} similarity spectra for fine-scale structures (FSS) and large-scale structures (LSS).³⁵ While these studies found relatively good agreement overall, two key spectral features in the measured data are not accounted for by the similarity spectra: the measured high-frequency slopes and peak-frequency characteristics for high engine power. After a description of the F-22A experiment and a review of these previous studies, the spectral characteristics at a variety of downstream and sideline distances are examined in a number of contexts, including their evolution with distance and additional comparisons against LSS and FSS similarity spectra. These results yield improved understanding of the radiated full-scale jet noise field, that in turn may eventually aid in reduction of source noise or personnel exposure.

II. Full-Scale Experiment Summary

An extensive experiment conducted at Holloman Air Force Base in July 2009 measured the noise produced by an F119-PW100 engine installed on a static F-22A Raptor. The engine nozzle exit is nominally rectangular, but the shape is influenced by the thrust vectoring paddles. The engine closest to the measurement microphones was cycled through four power conditions: idle, intermediate (80%), military (100%), and full afterburner, while the other engine was held at idle. Additional details regarding of the aerodynamics of the jet flow are not available. Although only a brief review of measurement procedures is given here, comprehensive descriptions may be found in Refs. 1 and 36.

Two microphone arrays were deployed for this experiment, the primary purpose of which was the first ever implementation of near-field acoustical holography on a military jet aircraft engine.⁷⁻⁹ However, this extensive data set has provided additional insights into the nature of the sound field in the vicinity of the aircraft, including weighted levels,³⁷ correlation,^{38,39} intensity,⁴⁰ equivalent source modeling,^{41,42} and shock content.²⁴ The first array consisted of 50 microphones on the ground, spaced 0.61 m (2 ft) apart and placed parallel to the engine's centerline at a sideline distance of 11.6 m (approximately 38 ft). Their locations are marked as dots in the schematic in Fig. 1. GRAS Type I microphones, ranging from 3.18 mm to 6.35 mm in diameter, were used in the ground-based line array, which spanned approximately 30 m in the z-direction – from 3 m upstream of the nozzle to 27.7 m downstream.

The second array of microphones is visible in the photographs in Fig. 2 and consisted of 90 Type I GRAS 40BE microphones arranged in a rectangular grid. The microphones were 15.2 cm (6.0 in) apart in both dimensions and covered an aperture 0.6 m high by 2.6 m long (2 ft x 8.5 ft). To form a large planar measurement aperture, the microphone rig was positioned at ten locations along a 22.9 m (75 ft)-long track (visible in Fig. 2). For a given plane of data, the rig was subsequently adjusted to three heights during the experiment, with the center of the array at 0.7, 1.3 and 1.9 m (27, 51, and 75 in). When the data from the 30 scans are pieced together, they yield a 1.8 m x 22.9 m (6 ft by 75 ft) measurement plane.

To obtain multiple planes of data, the track was moved to the different offset distances and three heights, as illustrated in Fig. 1. The red triangles along the track indicate the locations of the horizontal center of the microphone array for subsequent measurement scans. The total

aperture for the set of 30 measurements obtained 4.1 m and 5.6 m from the estimated shear layer of the jet plume are referred to as plane 1 and plane 2, respectively. Additionally, rig array measurements were taken in 10° increments at a center height of 1.9 m (75 in) along an arc 22.9 m (75 ft) centered at the estimated dominant source location (denoted by an “x” in Fig. 1), similar to that used in other full-scale experiments.^{29,30} This origin is in general accordance with various source characterization analyses including beamforming,²² collapse of waveform data along propagation radials,²⁹ near shear-layer power distribution,¹⁶ wave packets,⁴² and near-field acoustical holography.⁷⁻⁹ All data were collected³⁵ with a PXI-based acquisition system using 24-bit National Instruments 446x and 449x series cards at sampling rates of 96 kHz for idle, intermediate, and military power, and at 48 kHz for afterburner. The overall sound pressure levels (OASPLs) at afterburner are shown in the right plot of Fig. 1. All analyses in this paper are based on the afterburner data.

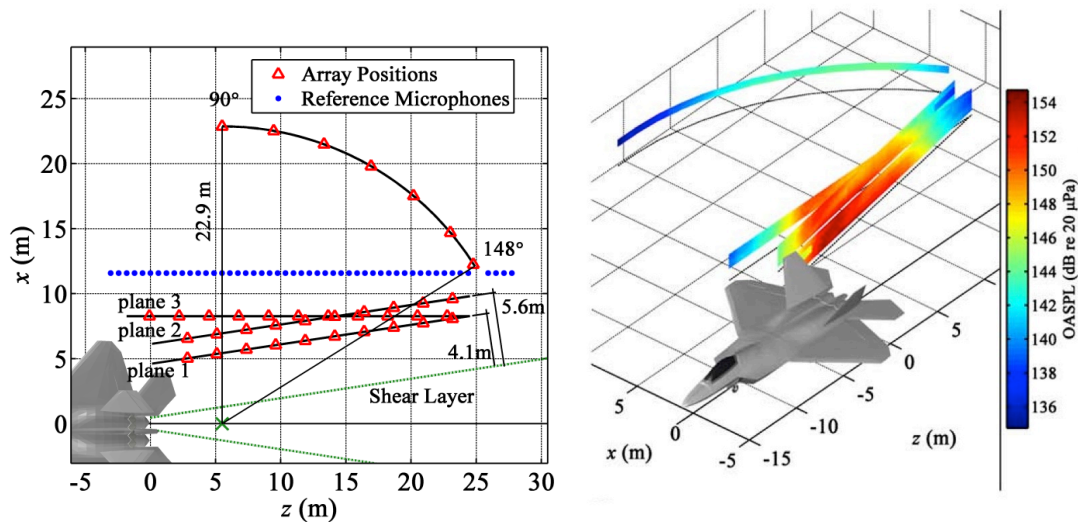


Figure 1. (Left) Schematic of the noise measurements taken near an F-22A Raptor at Holloman AFB July 2009. The triangles indicate the locations of the horizontal center of the 5x18 microphone field array during the experiment. The dots represent the locations of 50 ground-based microphones. All angles are measured relative to the engine inlet and to the estimated maximum source region shown as an x. (Right) Overall sound pressure level (OASPL) at afterburner on planes 1, 2 and 3 and the arc at 22.9 m (75 ft).



Figure 2. Photographs from F-22A test in 2009. The rectangular array of microphones with guide rail is shown near the aircraft. The ground-based microphone array is located just inside the edge of the pavement. A close up of the array is shown on the right.

III. Background/Previous work

While application of FSS and LSS similarity spectra to laboratory-scale jet noise has been extensive, only recently has the ability of the FSS and LSS to represent the noise from a high-performance military engine been explored. A review of many of the laboratory-scale studies is provided in Ref. 31. The first comparison of the LSS similarity spectrum to noise in the maximum radiation direction from an uninstalled, full-scale engine was reported by Schlinker *et al.*²² While reasonable agreement was found between the measured and LSS similarity spectra for low frequencies and in the peak-frequency region, they reported high-frequency slopes that were substantially shallower than those predicted by the LSS similarity spectrum. A similar shallow slope has been observed in laboratory measurements of supersonic jets, including those by Petitjean and McLaughlin,²⁵ Gee *et al.*,¹⁹ and Schlinker.³ An investigation³¹ of spectral shapes recorded on the ground-based microphones for the F-22A data set, discussed in the previous section, confirmed that for high engine powers, the measured high-frequency slope in the maximum direction is shallower than predicted by either the FSS or the LSS similarity spectra. In addition, the spectra measured at angles forward of the maximum radiation direction also have a shallower slope. The comparisons showed an additional discrepancy between the full-scale data and the similarity spectra: the measured spectra around the maximum radiation direction have a distinct double frequency peak.³¹

The conclusions drawn from the F-22A similarity-spectra analyses (shallower high-frequency slope and double-frequency peak) were evaluated by comparing the FSS and LSS similarity spectra to measurements from an unheated, laboratory-scale jet and the F-35AA³². For the laboratory-scaled jet, two cases were examined: ideally expanded subsonic (Mach 0.85) and supersonic (Mach 2.0) jets. The Mach 0.85 laboratory-scale jet spectra agree well with the similarity spectra. However, for the Mach 2.0 spectra, there is a clear lessening in high-frequency slope relative to the LSS spectrum around the maximum radiation direction. The slopes approach -10 dB/decade on one-third octave scales, rather than the -17.7 dB/decade predicted by the LSS spectrum.^{33,34} This discrepancy was investigated further in the context of the F-35AA analysis with the spectra measured at a distance of 38.1 m (125 ft) for three engine powers: 75%, 100% (military) and 150% (afterburner). Because the microphones were at a height of 1.5 m (5 ft), comparisons with the similarity spectra were complicated by the presence of ground reflections. However, for all three engine powers, reasonable agreement was achieved

between the FSS and the measured sideline spectrum and the LSS and the spectra measured farther aft with the same two exceptions found previously in the F-22A spectra. First, the high-frequency slopes of the measured spectra are shallower at a wide range of angles than the similarity spectra in the high-amplitude cases. Second, there is a double peak present in the F-35AA spectra in the maximum radiation region that is not predicted by the model and is not present in the laboratory-scale data.

As examples of both these features, the measured spectra along the ground-based array to the sideline of the F-22 are compared to the similarity spectra. Six downstream distances from $z = 0$ m (to the sideline of the nozzle exit) to $z = 25$ m are shown in Fig. 3. Although the analyses in this paper are described in terms of downstream distance, angles relative to the estimated maximum source location for these distances are provided in Table 1, in order to compare locations with the previous analyses in Refs. 31 and 32. The more rounded FSS similarity spectrum is shown to provide a reasonable approximation to the spectra measured at $z = 0$ m except for the shallower measured slope above about 3 kHz. At $z = 5$ m, the FSS spectrum matches the overall shape of the spectrum (except for the shallower high frequency slope), but the LSS contributes to the peak region, such that a combination of the two provides a better prediction of the measured spectra. The more peaked LSS similarity spectrum fits the measured spectra at $z = 10$ m and 15 m, except for the slope above about 1 kHz. In addition, in the $z = 15$ m case, there is a distinct double frequency peak (in the 125 and 250 Hz OTO bands) in the measured spectrum that is not accounted for in the model. Farther aft of the maximum region, at $z = 20$ m, the LSS provides a good fit for the measured data over the entire frequency range of interest. However, beyond this distance, at $z = 25$ m, the high-frequency portion of the spectral shape changes such that a combination of the LSS and the FSS similarity spectra represent the measured spectra better than the LSS alone. This was first noted in Ref. 31, where it was shown that while the addition of this FSS component does not contribute significantly the OASPL, the measured spectral shape far aft of the maximum region appears to exhibit a combination of LSS and FSS similarity spectral shapes.

Table 1. Downstream distances considered in this paper and angles, relative to engine inlet and referenced to the estimated maximum source region in Fig. 1.

| Downstream distance, z | 0 m | 5 m | 10 m | 15 m | 20 m | 25 m |
|--------------------------|-----|-----|------|------|------|------|
| θ at ground array | 65° | 87° | 110° | 130° | 142° | 148° |
| θ at plane 1 | 51° | 85° | 126° | 144° | 152° | 156° |
| θ at plane 2 | 58° | 86° | 121° | 139° | 148° | 153° |
| θ at arc | | 89° | 101° | 113° | 129° | 149° |

Another way to examine the presence of the double peaks in the measured spectra is to view the change in spectral content with downstream distance across all 50 ground-based microphones, located 11.6 m to the sideline of the F-22A (see Fig. 1). To provide a more consistent result, the spectra recorded for 30 afterburner runups are averaged and shown as a function of downstream distance in Fig. 4. Of particular importance to the present work is the evidence of a double peaks in the spectra around the $z = 7$ -17 m range. Over these downstream distances, the relative contribution of discrete frequency components shifts resulting in the

double peak observed at individual measurement locations. This causes the maximum frequency to stay constant over a certain distance and then transition to the next lower peak. Although OTO peak frequencies are discrete by nature, note that 200 Hz and 315 Hz do not appear as the peak frequencies at any downstream distance. On an OTO scale, there are three clearly distinguishable bands, at 800, 250, and 125 Hz, as distance is increased downstream. A fourth band, corresponding to 400 Hz, is also visible in the data but is less distinct. It is also possible that another band at 80 Hz, exists, but this would be clearer had the aperture been extended farther downstream. These bands, in particular the first three, are readily visible in the right plot of Fig. 4, which shows the OTO peak frequency (red dots) and 3-dB down frequencies (black error bars) versus downstream distance. After a frequency transition, the peak frequency remains constant when moving downstream while the width of the peak-frequency region increases because of the increasing contribution of the second peak. After the lower-frequency peak overtakes the higher-frequency peak in amplitude, a sudden transition occurs. The reason for this double peak in the spectrum is not fully understood at the present, but it is present in both F-35AA and F-22A data. As discussed previously, the characteristics of the shallower high-frequency slope and the nature of the double peak at different ranges in the geometric near field constitute the focus of this paper.

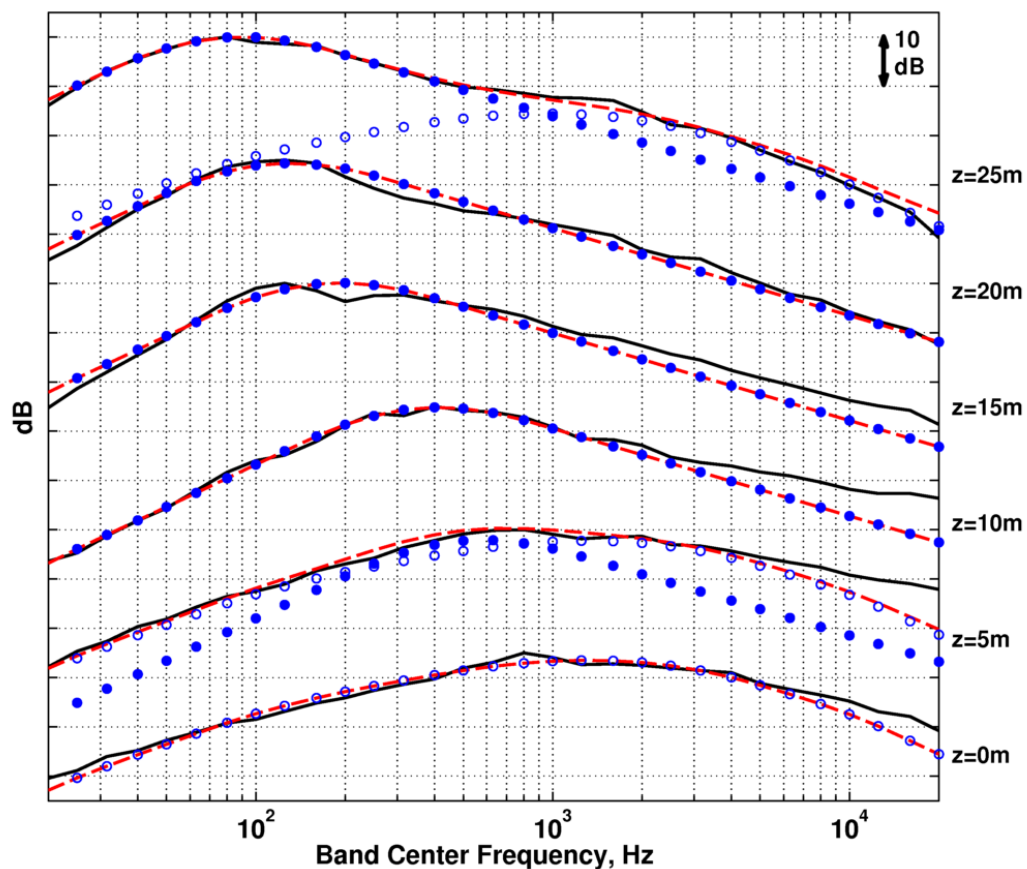


Figure 3. One-third octave sound pressure levels recorded at ground-based microphones for afterburner (solid lines), at the downstream distances indicated, compared to the total similarity spectrum match (dashed lines) and the contributions of the LSS (filled circles) and the FSS (open circles) similarity spectra. Each spectra is shifted by 25 dB.

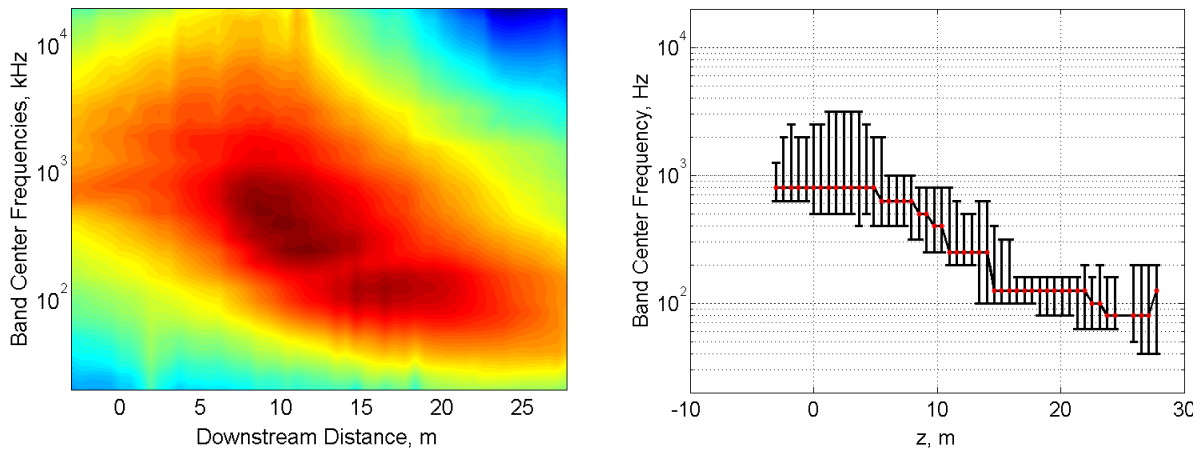


Figure 4. (Left) One-third octave sound pressure levels at afterburner over the downstream distance on the ground-based microphones 11.6 m to the sideline. (Right) The corresponding peak OTO band frequencies (red dots), along with the upper and lower 3 dB down points (black vertical bars).

IV. Near-field Spectral Analysis

To further investigate the high-frequency slope and the double peak of the spectra measured in the vicinity of the F-22, data recorded on the rectangular microphone array at planes 1 and 2 and along the arc (shown in Fig. 1) are analyzed. The geometry of the measurement planes facilitates an investigation into the variation of these features with respect to both downstream and sideline distance. However, because the extended nature of the source and the proximity to the aircraft make analysis along observation radials nonintuitive, the analyses are simply referenced relative to downstream direction, z . Before the results are presented, two considerations regarding the location and orientation of the rig microphones are addressed.

First, because of the locations of the field array microphones, the rigid ground plane introduces significant range and height-dependent interference features into the spectra. Figure 5 illustrates this effect for the 13 microphones [at heights of 0.15 m (0.5 ft) to 2.21 m (7.25 ft)] at downstream distances of 5 and 20 m on plane 2. The microphones at $z = 5$ m, which are to the sideline of the estimated maximum source region (see Fig. 1), show evidence of destructive interference from approximately the 125 Hz to 1000 Hz one-third-octave bands. These are similar to the frequencies (150 Hz to 2 kHz) at which nulls would occur for a monopole located at the estimated peak source location along the jet centerline, but the interference effects are relatively mild because of the extended volumetric nature of the source and the frequency band integration. This is particularly true at $z = 20$ m because the source is being observed somewhat end-on, with contributions of energy from many locations. Consequently, the interference nulls are minimal in nature, particularly for the lowest microphones, which can be considered effectively on the ground plane for the frequencies of interest. However, because locations closer to the sideline have stronger interference effects, an average of the spectra for the 13 microphones for a given downstream distance, z , is used in the analyses to mitigate the ground reflection effects and to investigate the high-frequency slopes and the peak-frequency regions of the spectra. It should be noted that the levels at both the low and high frequencies are consistent across the 13 microphone heights.

The second microphone consideration is the orientation of the GRAS 40BE free-field rig microphones located on the rig. Because the microphones were oriented perpendicular to the rig

track (the straight lines in Fig. 1), the angle of incidence varied significantly as the array was moved to subsequent scan locations. Because free-field microphones are designed for normal incidence, the angular variation results in a required high-frequency spectra correction that exceeds 1 dB (for grazing incidence) above 10 kHz. This correction is minor, with the greatest correction being only ~ 3 dB at 20 kHz for the locations farthest downstream, but was included to provide consistency with the arc data, where the microphones were pointed towards the estimated source region (see Fig. 1).

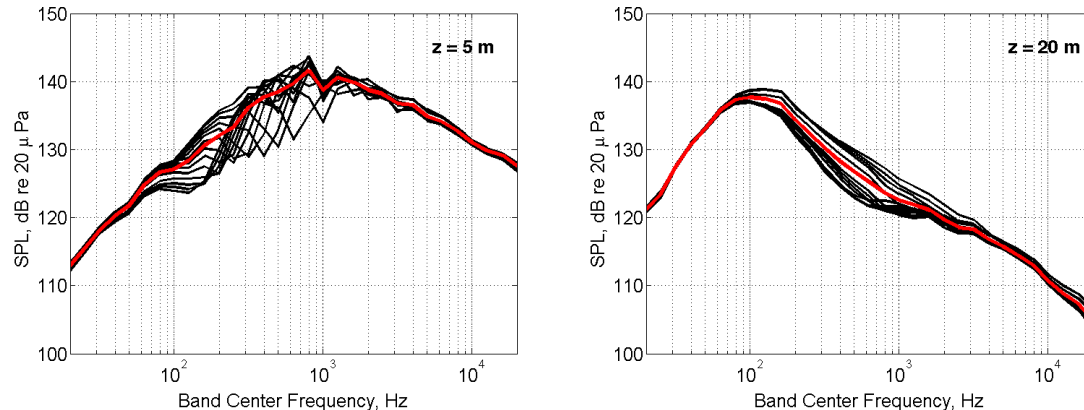


Figure 5. One-third octave band sound pressure levels at afterburner on plane 2 at $z = 5$ m (left) and 20 m (right). The black lines correspond to the spectra on the 13 microphones with heights from 0.15 m (0.5 ft) to 2.21 m (7.25 ft) at each downstream distance. The red line is the average of the 13 spectra and is referred to as the height-averaged spectrum.

A. High-frequency spectral slope

As was shown in Fig. 3, the most notable difference between the similarity spectra and the noise recorded at the ground-based microphones at high engine power is the slope of the high-frequency portion of the spectra. Evidence that this slope changes with angle and engine condition is given in Ref. 31. Similar discrepancies have been found for spectra from the F-35AA at 38 m and Mach 2.0 laboratory-scale data³² and in far-field data for the F-22A for both measured and modeled nonlinear propagation effects.²⁹ Because of the inability to model nonlinear propagation in simple fashion in the geometric near field, a measured high-frequency spectral slope analysis is useful. The data from plane 1 and plane 2 for one engine operating at afterburner are used to further investigate the changes in the high-frequency slope as a function of downstream and sideline distance.

Because the dominant ground interference effects occur below a few kilohertz, the high-frequency spectral slope is calculated for the height-averaged spectra over the two-octave band of 5-20 kHz. This slope is then converted to dB/decade by multiplying by a factor of 5/3 to account for the number of one-third octave bands in a decade. The resulting high-frequency slope along planes 1 and 2 is shown in Fig. 6 as a function of downstream distance. For convenience, lines demarcating -10 dB/decade and -17.7 dB/decade are shown. The -10 dB/decade is the high-frequency slope that corresponds to the $1/f^2$ limit for OTO spectra calculated from shock-containing waveforms.⁴³ The -17.7 dB/decade slope is the OTO version of the high-frequency slope of the Tam *et al.* LSS similarity spectra.^{33,34} Note that for narrowband spectra, the slopes would roll off faster, at an additional 10 dB/decade.

The high-frequency slopes on planes 1 and 2 vary significantly with downstream distance, as seen in Fig. 6. For locations to the side of the engine (the smallest z), it is possible that the high-frequency slope of less than -10 dB/decade may be attributed to scattering and/or shielding

effects caused by the aircraft, but it could also be source related. As distance increases, there is a general decrease in the high-frequency slope (steepening of the roll-off), but there are some points of special interest. First, for $z \sim 5-10$ m downstream of the nozzle, the high-frequency slope is essentially pinned at the $1/f^2$ limit. Although by itself, a $1/f^2$ slope is not incontrovertible evidence of nonlinear propagation, it is the expected slope when the shocks are forming via waveform steepening. Second, as distance increases, the slope decreases, but the slope on plane 2 for $z \sim 10-17$ m is significantly shallower than plane 1. The evident change to a shallower slope at larger propagation distances is very likely attributable to nonlinear waveform steepening, although the slope has not reached the shock-induced -10 dB/decade limit for $z > 13$ m. These results, coupled with concurrent²⁴ and previous²⁹ analyses, indicate that significant nonlinear evolution and shock strengthening occurs in the geometric near field and extends to the far field.

Beyond the maximum amplitude region, there is a much slower evolution of spectral slope between planes 1 and 2. Around $z = 18-20$ m, the slope flattens out briefly near the -17.7 dB/decade associated with the LSS similarity spectra, then for $z > 20$ m decreases again, meaning that the spectra have a steeper roll-off than the Tam *et al.* LSS similarity spectra. Although Fig. 6 is a convenient way of compiling these results, a closer examination of the spectra in each of these regimes gives additional insights.

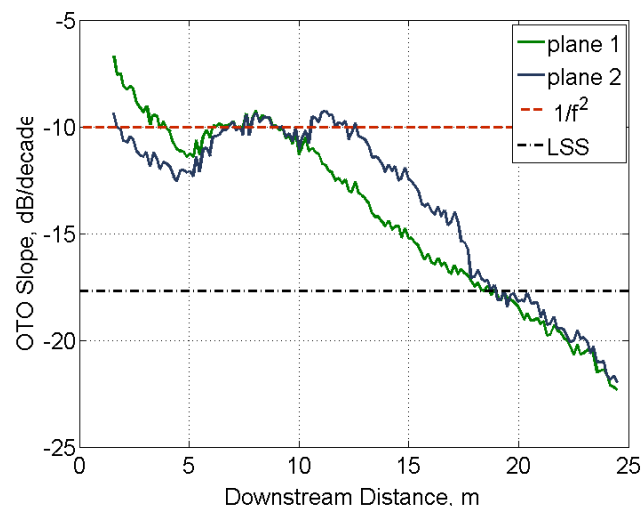


Figure 6. High-frequency slopes of the height-average spectra along planes 1 and 2. The $1/f^2$ limit of -10 dB/decade is displayed as a red dashed line, and the -17.7 dB/decade slope of the OTO LSS similarity spectrum is shown as a black dash-dotted line.

Figure 7 displays the OTO height-averaged spectra for downstream distances of $z = 0, 5, 10,$ and 15 m on planes 1 and 2 and the arc at 22.9 m (75 ft) for $z \geq 5$ m. The arc data are included to give an indication of how the spectra evolve with distance, but note that the sideline distance between plane 2 and the arc decreases with increasing downstream distance. The corresponding sideline distances can be seen in Fig. 1. In the arc data, which represents a constant distance from the estimated dominant aeroacoustic origin, there is a broad ground interference null around $500 - 800$ Hz at all four downstream distances. Although the depth of the null is decreased by averaging over the five microphones, the location in frequency of the null corresponds again to that predicted for a monopole source along the jet centerline at the estimated origin and a microphone at 1.9 m, the height of the center of the array. To the sideline of the nozzle exit,

$z = 0$ m, the spectra on planes 1 and 2 have an initial shallower slope than the -10 dB/decade, which is illustrated by the dashed red lines. Although scattering due to the aircraft body may be a real possibility, the spectra are relatively smooth. As was evident in Fig. 6, the high-frequency slope has steepened slightly from plane 1 to plane 2.

At $z = 5$ m, which is to the sideline of the estimated maximum source region, the high-frequency slope on planes 1 and 2 and the arc are all approximately -10 dB/decade. The peak frequencies for all three cases are similar, except for the interference null on the arc, which likely indicates that at least the high frequency noise is propagating radially along this line. This provides additional confirmation as to the choice of the aeroacoustic origin, as the maximum OASPL-producing region is upstream of the dominant source regions at low frequencies.^{1,23} The change in high-frequency levels from plane 1 to the arc is approximately 16 dB, which is close to the 15 dB predicted by spherical spreading from a monopole located at the edge of the shear layer at the jet centerline height. It is reasonable to assume that the noise along the $z = 5$ m direction is spreading in a spherical manner because this sideline radiation is primarily accounted for by the FSS (see Fig. 3), which are believed to be relatively compact sources.

The remaining plots in Fig. 7 represent two measurement locations farther downstream, at $z = 10$ and 15 m. At $z = 10$ m, which was the largest distance downstream for which the spectra had the -10 dB/decade slope at plane 1 (see Fig. 6), all three spectra are seen to have the -10 dB/decade slope, which is noted by the dashed red line. At $z = 15$ m, the slope becomes slightly shallower as sideline distance increases from plane 1 to the arc, which has a slope of, again, -10 dB/decade. While the noise does not propagate outward perpendicularly from the centerline, (i.e., these do not represent propagation radials, with the possible exception of the ~ 5 m downstream location), the greater sideline distances represent longer propagation paths from the source region for waveform steepening and high-frequency nonlinear energy transfer to occur.

Although the primary purpose of this analysis is to examine the shallower high-frequency slope in the measured data than predicted by the LSS spectra, the behavior of the spectra farther downstream also merit further examination. If the high-frequency slope results in Figure 6 are revisited, we see that at $z > 18$ m, the slopes on the two planes are similar and that at $z \approx 18 - 20$ m, the slopes are close to that of the LSS similarity spectrum. However, for greater downstream distances, the slopes of the measured spectra are steeper. To illustrate the difference between these two cases, plane 2 spectra at $z = 20$ and 25 m are displayed in Fig. 8, along with similarity spectra matches, similar to those carried out in Refs. 31 and 32. In addition to the height-average spectrum, the spectra recorded on the top ($y = 0.15$ m) and bottom ($y = 2.21$ m) microphones of the rectangular array are also shown. The purpose of including the three spectra is to show how ground interference nulls are not nearly as significant far downstream, especially on the lowest microphone, because of the geometry and the volumetric nature of the source. This lends further validity to attempting similarity spectra matches. At $z = 20$ m (see Fig. 8), the LSS similarity spectrum is shown to match the low and peak frequency regions. However, it does not agree with the high-frequency region of the measured spectrum, even though the slope of the average spectrum in the 5-20 kHz band is approximately the same.

For larger downstream distances, Fig. 6 showed that the the high-frequency slope continues to decrease, corresponding to a steeper high-frequency roll-off than is predicted by the LSS similarity spectrum. This occurs, in part, because the slope itself no longer follows a power-law roll-off, as can be seen in Fig. 8. It was first shown in Ref. 31 that the afterburner spectral shape at the ground-based microphones for 150° is better represented by a combination of the LSS and

FSS similarity spectra. Similar behavior was also observed in F-35AA data near 148° .³² The shape of the spectra here, whether at the top, bottom, or averaged along the rig, suggest that the spectra at $z = 25$ m along plane 2 can also be represented by an FSS/LSS combination, except for the apparent flattening of the measured spectra at the peak frequency region. The close agreement between the similarity spectra and measured spectra in Fig. 8 could indicate that directly behind the maximum radiation area, the large-scale structures account for the noise radiation only, but farther aft, where the peak level is substantially lower, the fine-scale structures may also influence the spectral content.

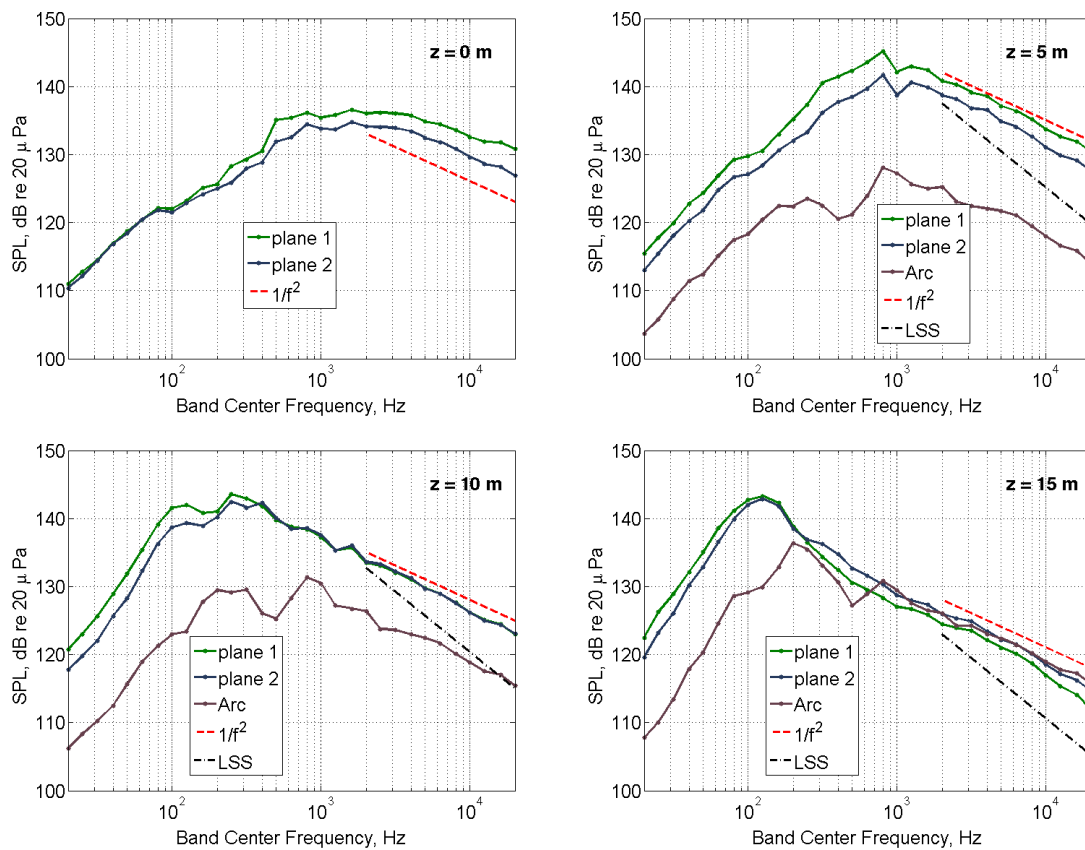


Figure 7. One-third-octave, height-averaged sound pressure levels at afterburner on plane 1 (green), plane 2 (blue), and the arc (purple) at downstream distances of 0 m (upper right), 5 m (upper left), 10 m (lower right) and 15 m (lower left). For comparison, the $1/f^2$ limit of -10 dB/decade is displayed as red dashed lines, and the -17.7 dB/decade slope of the OTO LSS similarity spectrum is shown as black dash-dotted lines.

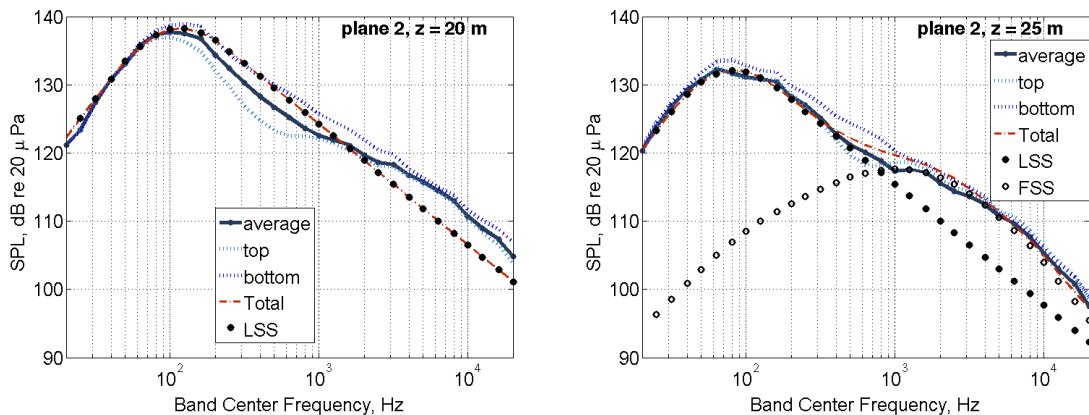


Figure 8. Comparison of the one-third-octave sound pressure levels at afterburner on plane 2 (blue) at downstream distances of 20 m (left) and 25 m (right) to the similarity spectra. The LSS similarity spectrum is shown as filled black circles, and the FSS similarity spectrum as empty black circles. The total predicted similarity spectrum, the sum of the LSS and FSS contributions, is shown as the red dashed line for $z = 25$ m.

B. Peak-frequency variation

A spectral feature exhibited for full-scale, high performance engines that is not present in laboratory-scale jet noise,³² is the presence of a double peak in the spectrum. This was visible at certain angles in Fig. 3 and in the two-dimensional spectral map in Fig. 4. Furthermore, instead of a continuous decrease in peak frequency as downstream distance increases, there appear to be discrete transitions in OTO frequency with the maximum level that arise because of the changing amplitudes of the double-peak components. The spatial variation of the OTO spectra measured on planes 1 and 2 near the F-22A provides additional insights into the nature of the double peak. Figure 9 displays the height-averaged spectra on plane 1 (upper left) and plane 2 (lower left). On both planes, there is a double-peak nature to the spectra in the region around $z \sim 8 - 13$ m downstream. Examination of the OASPL displayed on the right side of Fig. 1 shows that this region corresponds to the maximum radiation direction. Again, this is caused by the relative growth and decay of discrete spectral components with distance downstream.

A closer look at the variation in peak frequency is given in Fig. 9 for plane 1 (upper right) and plane 2 (lower right). The red dots show the band center frequency of the maximum level, and the black lines indicate band center frequencies at which the level is within 3 dB of the maximum. While the expected trend of a shift from higher to lower peak frequency as downstream distance increases is manifest, it is noteworthy that for approximately $6 \text{ m} < z < 17$ m on plane 1 and $7 \text{ m} < z < 19$ m on plane 2, the peak band center frequency changes discretely from 400 Hz to 250 Hz to 125 Hz. It is significant that the peak energy is constrained to a narrow bandwidth around 125 Hz for a long downstream distance (approximately 12-18 m on plane 2) before shifting to lower frequencies farther aft. This narrow 3-dB-down bandwidth centered around 125 Hz corroborates the observed spectral shapes on the ground-based microphone data, as was shown in Fig. 4.

To further investigate the double-peaked spectral shapes and discrete transitions in peak frequency, the sound field measured at plane 1 and the arc at 22.9 m (75 ft) at frequencies of interest are displayed in Fig. 10. The selected frequencies 125 Hz, 250 Hz, 400 Hz, and 800 Hz are the peak frequencies across large portions of the ground-based array (see Fig. 4) and planes 1 and 2 (see Fig. 9). The radiation patterns for these frequencies along plane 1 show markedly

different “source” regions. These regions are listed in Table 2 and correspond with relatively large changes in apparent directivity. While these cannot be referred to as actual directivities because the measurements are not in the far field, the relative comparisons are useful. The double-peak nature of the spectra appears to result from these different directivities contributing different amounts to the measured noise as they slice through a given (x, z) location. However, this does not explain the discrete nature of the frequency transitions, nor why similar behavior is not seen in laboratory-scale measurements. Note that we did attempt to model the double-peak behavior using two LSS spectra with different peak frequencies, but were unsuccessful because the peak frequencies are so closely spaced as to alter the overall spectral shape when the contributions are summed. Consequently, we can conclude that the double peaks are not evidence of independent LSS contributions to the spectrum at a given measurement location, at least not as the LSS spectrum has been defined by Tam *et al.*^{33,34} Further investigation based on partial field decomposition⁸ and near-field acoustical holography⁷ could lead to an improved understanding of these spectral features that appear to be unique to high-performance, full-scale jet noise.

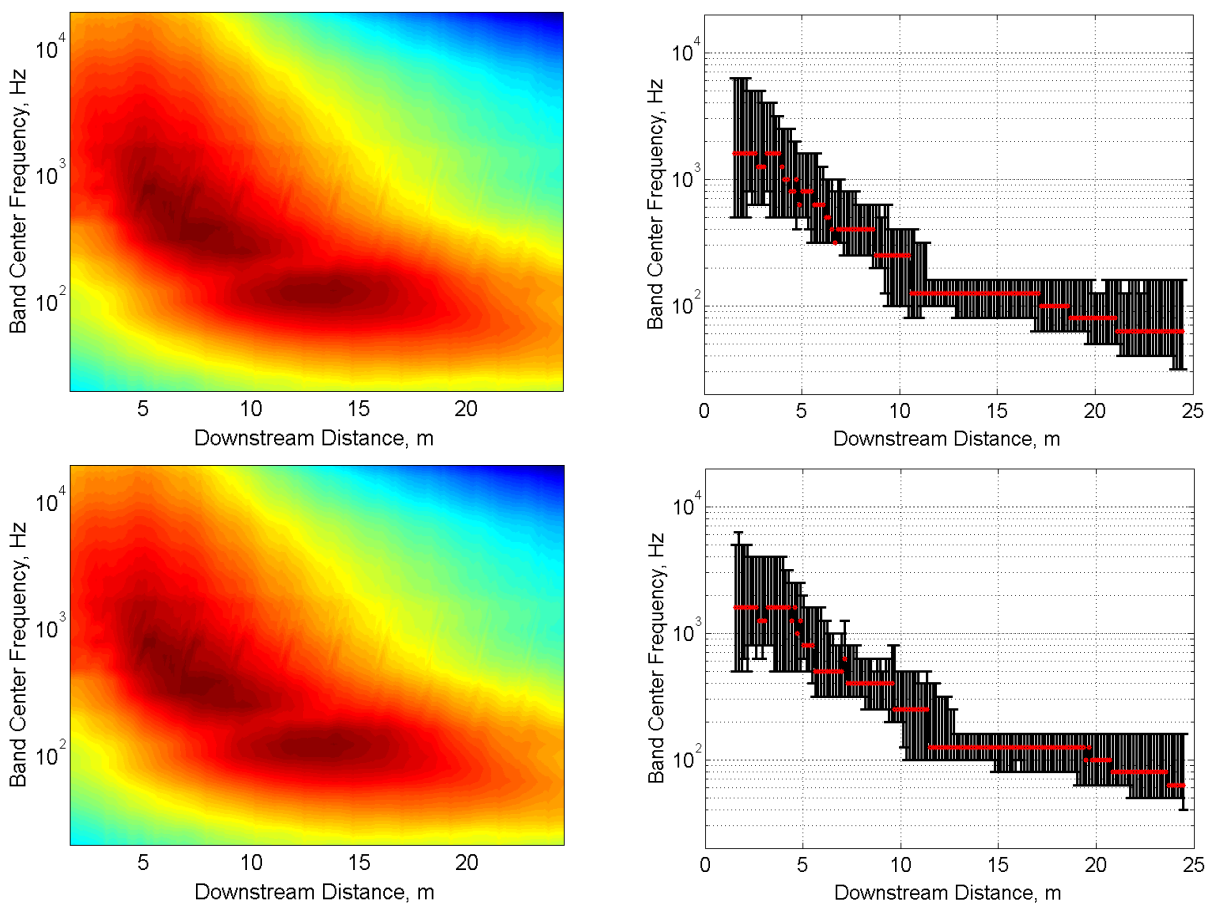


Figure 9. One-third octave height-averaged sound pressure levels over the downstream distance on plane 1 (upper left) and plane 2 (lower left). The corresponding peak OTO band frequencies (red dots) along plane 1 (upper right) and plane 2 (lower right), along with the upper and lower 3-dB down points (black vertical bars).

Table 2. Locations of maximum level and the 3-dB-down points for the SPL, shown in Fig. 10, on plane 1 and the arc at 22.9 m at the primary peak frequencies.

| | 125 Hz | 250 Hz | 400 Hz | 800 Hz |
|----------------|----------------------------|----------------------------|----------------------------|---------------------------|
| Plane 1 | 13.8 m (10.0 m, 16.5 m) | 8.8 m (6.2 m, 11.8 m) | 7.7 m (5.3 m, 10.0 m) | 5.0 m (4.4 m, 7.7 m) |
| Arc | 21.2 m (19.2 m, 24.2 m) | 15.9 m (13.7 m, 19.3 m) | 14.5 m (12.1 m, 21.2 m) | 13.2 m (8.8 m, 14.5 m) |

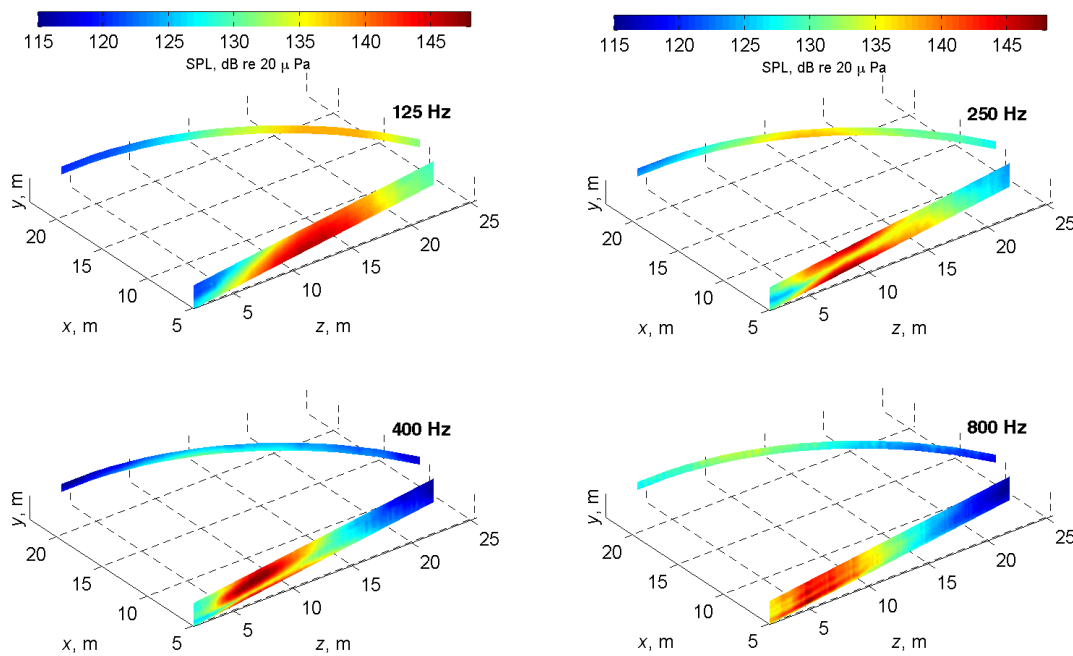


Figure 10. One-third-octave band sound pressure levels for afterburner along plane 1 and the arc at 22.9 m (75 ft) at 125 Hz (upper left), 250 Hz (upper right), 400 Hz (lower left), and 800 Hz (lower right). All plots have the same color scale.

IV. Concluding Summary

This paper has extended previous analyses of the spectral characteristics of noise near high-performance jet engines.^{22,31,32} Neilsen *et al.*^{31,32} showed previously that the Tam *et al.*^{33,34} fine and large-scale similarity spectra match the overall shape of measured spectra for a full-scale engine at high power quite well, with notable two exceptions: a shallower measured high-frequency slope at some angles and the presence of a double peak in the measured spectrum. Although the shallower high-frequency slope is also present in supersonic, laboratory-scale jet data, the double spectral peak appears to be unique to full-scale jets. These spectral features have been further investigated in this paper by examining additional portions of the overall F-22A measurement¹ than considered previously.

As part of the analysis, the variation in high-frequency slope with downstream and sideline distances has been evaluated more quantitatively than before. At the farther measurement plane (plane 2), the spectra associated with the maximum radiation region have slopes close to the -10 dB/decade slope associated with the $1/f^2$ dependence expected when shocks are present. This is noteworthy because it indicates that significant nonlinear steepening of the waveforms is happening in these areas, before the transition to far-field nonlinear propagation.^{29,30} At distances aft of the maximum radiation region, there is an aperture over which the slope matches that of the LSS similarity spectra. However, farther aft, the slope continues to decrease, indicative of a physical change in the spectral shape. The dependence of the high-frequency slope on location has implications in understanding fundamental properties of jet noise radiation. It is clear that although the Tam *et al.*^{33,34} similarity spectra are useful models in describing large and fine-scale features of the noise radiation, including the potential presence of both components far downstream, they cannot account for this important aspect of the noise radiation – that of an evolving high-frequency slope due to nonlinear propagation. It is unclear how these models can be corrected, given that nonlinearity will change with engine condition, distance, and radiation angle.

The double-peaked nature of the F-22A spectra also indicate an important deviation from the similarity spectra models. The present analysis of the peak-frequency region of the spectral shapes has added support to previous observations that this is one way in which high power, full-scale jets differ from supersonic, laboratory-scale jets. It appears fundamentally important that peak frequency does not vary continuously with downstream distance, but rather transitions in discrete intervals as the result of the relative contributions of different spectral components. Further exploration is being conducted using partial field decomposition⁸ and near-field acoustical holography.⁷ These analyses provide additional understanding of the noise radiation characteristics near the engine. They also point to the need for better matching between laboratory-scale experiments and numerical simulations and the full-scale conditions they are meant to model. Improved matching based on enhanced understanding will allow for more effective noise mitigation and reduction strategies and technologies to be developed.

Acknowledgments

The authors gratefully acknowledge funding from the Office of Naval Research. The measurements were funded by the Air Force Research Laboratory through the SBIR program and supported through a Cooperative Research and Development Agreement (CRDA) between Blue Ridge Research and Consulting, Brigham Young University, and the Air Force. Distribution A – Approved for Public Release; Distribution is Unlimited (88ABW-2013-2271).

References

- ¹Wall, A. T., Gee, K. L., James, M. M., Bradley, K. A., McInerney, S. A., and Neilsen, T. B., “Near-field Noise Measurements of a High-power Jet Aircraft,” *Noise Control Engineering Journal*, Vol. 60, 2012, pp. 421-434.
- ²Bridges, J. and Wernet, M. “Measurements of the Aeroacoustic Sound Source in Hot Jets,” NASA/TM – 2004-212508, NASA Glenn Research Center, Cleveland, OH, Feb. 2004.
- ³Schlinker, R. H., “Supersonic Jet Noise Experiments,” Ph.D. Dissertation, Department of Aerospace Engineering, University of Southern California, 1975.
- ⁴Laufer, J., Schlinker, R. H., and Kaplan, R. E., “Experiments on Supersonic Jet Noise,” *AIAA Journal*, Vol. 14, 1976, pp. 489-497.
- ⁵Tam, C. K. W., Viswanathan, K., Ahuja, K. K., and Panda, J. “The Sources of Jet Noise: Experimental Evidence,” *Journal of Fluid Mechanics*, Vol. 615, 2008, pp. 253-292.

- ⁶Lee, M. and Bolton, J. S., "Source Characterization of a Subsonic Jet by Using Near-field Acoustical Holography," *Journal of the Acoustical Society of America*, Vol. 121, 2007, pp. 967-977.
- ⁷Wall, A. T., Gee, K. L., Neilsen, T. B., Krueger, D. W., James, M. M., Sommerfeldt, S. D., and Blotter, J. D., "Full-scale Jet Noise Characterization Using Scan-based Acoustical Holography," AIAA Paper 2012-2081.
- ⁸Wall, A. T., Gee, K. L., Neilsen, T. B., and James, M. M., "Partial Field Decomposition of Jet Noise Sources Using Optimally Located Virtual Reference Microphones," *Proceedings of Meetings on Acoustics*, Vol. 18, 2012, paper 045001.
- ⁹Wall, A. T., "The Characterization of Military Aircraft Jet Noise Using Near-field Acoustical Holography," Ph.D. Dissertation, Department of Physics and Astronomy, Brigham Young University, Provo, UT, April 2013.
- ¹⁰Shah, P.N., Vold, H. and Yang, M., "Reconstruction of Far-Field Noise Using Multireference Acoustical Holography Measurements of High-Speed Jets," AIAA paper 2011-2772.
- ¹¹Suzuki, T. and Colonius, T., "Instability Waves in a Subsonic Round Jet Detected Using a Near-field Phased Microphone Array," *Journal of Fluid Mechanics*, Vol. 565, 2006, 197-226.
- ¹²Schlinker, R., Simonich, J. C., Reba, R. A., Colonius, T., and Ladeinde, F., "Decomposition of High Speed Jet Noise: Source Characteristics and Propagation Effects," AIAA Paper 2008-2890.
- ¹³Reba, R. A., Simonich, J. S., and Schlinker, R. H., "Chevron Nozzle Effects on Wavepacket Sources in a Supersonic Jet," AIAA Paper No. 2012-2253.
- ¹⁴Yang, M. Y., Vold, H., and Shah, P., "Measurement and Propagation of Supersonic Aeroacoustics Noise Sources Using Continuous Scanning Measurement Technologies and the Fast Multipole Boundary Element Method," *Proceedings of Meetings on Acoustics*, Vol. 14, 2011, paper 040001.
- ¹⁵Tam, C. K. W., Viswanathan, K., Pastouchenko, N. N. and Tam, B. "Continuation of the Near Acoustic Field of a Jet to the Far Field. Part II: Experimental Validation and Noise Source Characteristics," AIAA Paper 2010-2729.
- ¹⁶Yu, J. C. and Dosanjh, D. S., "Noise Field of a Supersonic Mach 1.5 Cold Model Jet," *Journal of the Acoustical Society of America*, Vol. 51, 1972, pp. 1400-1410.
- ¹⁷Baars, W. J., Tinney, C. E. and Woche, M. S., "Nonlinear Noise Propagation from a Fully Expanded Mach 3 Jet," AIAA Paper 2012-1177.
- ¹⁸Baars, W. J., Tinney, C. E., Murray, N. E., Jansen, B. J., and Praveen, P., "The Effect of Heat on Turbulent Mixing Noise in Supersonic Jets," AIAA Paper 2011-1029.
- ¹⁹Gee, K. L., Atchley, A. A., Falco, L. E., Shepherd, M. R., Ukeiley, L. S., Jansen, B. J., and Seiner, J. M., "Bicoherence Analysis of Model-scale Jet Noise," *Journal of the Acoustical Society of America*, Vol. 128, 2010, pp. EL211-216.
- ²⁰Gee, K. L., Neilsen, T. B., and Atchley, A. A., "Near-field Skewness in Laboratory-scale Supersonic Jet Data," *Journal of the Acoustical Society of America*, 2013.
- ²¹Mora, P., Heeb, N., Kastner, J., Gutmark, E. J., and Kailasanath, K., "Near and Far field Pressure Skewness and Kurtosis in Heated Supersonic Jets from Round and Chevron Nozzles," Proc. ASME Turbo Expo 2013, GT2013-95774, June 2013.
- ²²Schlinker, R. H., Liljenberg, S. A., Polak, D. R., Post, K. A., Chipman, C. T., and Stern, A. M., "Supersonic Jet Noise Source Characteristics & Propagation: Engine and Model Scale," AIAA Paper 2007-3623 (May 2007).
- ²³Gee, K. L., Neilsen, T. B., Downing, J. M., James, M. M., McKinley, R. L., McKinley, R. C., and Wall, A. T., "Near-field Shock Formation in Noise Propagation from a High-power Jet Aircraft," *Journal of the Acoustical Society of America*, Vol. 133, 2013, EL88 – EL93.
- ²⁴Gee, K. L., Neilsen, T. B., Muhlestein, M. B., Wall, A. T., Downing, J. M., James, M. M., and McKinley, R. L., "On the Evolution of Crackle in Jet Noise from High-Performance Engines," AIAA Paper 2013-2190.
- ²⁵Petitjean, B. P. and McLaughlin, D. K. "Experiments on the Nonlinear Propagation of Noise from Supersonic Jets," AIAA Paper 2003-3127.
- ²⁶Gallagher, J. A. and McLaughlin, D. K., "Experiments on the Non-linear Characteristics of Noise Propagation from Low and Moderate Reynolds Number Supersonic Jets," AIAA Paper 81-2041, Oct. 1981.
- ²⁷Petitjean, B. P., Viswanathan, K. and McLaughlin, D. K., "Acoustic Pressure Waveforms Measured in High Speed Jet Noise Experiencing Nonlinear Propagation." *International Journal of Aeroacoustics*, Vol. 5, 2006, pp. 193-215.
- ²⁸Viswanathan, K., Alkislar, M. B., and Czech, M. J., "Characteristics of the Shock Noise Component of Jet Noise," AIAA Journal, Vol. 48, 2010, pp. 25-46.
- ²⁹Gee, K. L., Sparrow, V. W., James, M. M., Downing, J. M., Hobbs, C. M., Gabrielson, T. B., and Atchley, A. A., "The Role of Nonlinear Effects in the Propagation of Noise from High-Power Jet Aircraft," *Journal of the Acoustical Society of America*, Vol. 123, 2008, pp. 4082-4093.
- ³⁰Gee, K. L., Downing, J. M., James, M. M., McKinley, R. L., McKinley, R. C., Neilsen, T. B., and Wall, A. T., "Nonlinear Evolution of Noise from a Military Jet Aircraft During Ground Run-up," AIAA Paper 2012-2258.
- ³¹Neilsen, T. B., Gee, K. L., Wall, A. T., and James, M. M., "Similarity Spectra Analysis of High-performance Jet Aircraft Noise," *Journal of the Acoustical Society of America*, Vol. 133, 2013, pp. 2116-2125.
- ³²Neilsen, T. B., Gee, K. L., Wall, A. T., James, M. M., and Atchley, A. A., "Comparison of Supersonic Full-scale and Laboratory-scale Jet Data and the Similarity Spectra for Turbulent Mixing Noise," *Proceedings of Meetings on Acoustics*, Vol. 19, 2013, paper 040071
- ³³Tam, C. K. W., Golebiowsky, M. and Seiner, J. M., "On the Two Components of Turbulent Mixing Noise from Supersonic Jets," AIAA Paper 96-1716.
- ³⁴Tam, C. K. W. and Zaman, K., "Subsonic Noise from Nonaxisymmetric and Tabbed Nozzles," *AIAA Journal*, Vol. 38, 2000, pp. 592-599.

- ³⁵Tam, C. K. W., "Mach Wave Radiation from High-Speed Jets," *AIAA Journal*, Vol. 47, 2009, pp. 2440 – 2448.
- ³⁶James, M. M. and Gee, K. L., "Aircraft Jet Plume Source Noise Measurement System," *Sound and Vibration*, Vol. 44, 2012, pp. 14-17.
- ³⁷Reynolds, S. C., Myres, J. S., Neilsen, T. B., Wall, A. T., Gee, K. L. and James, M. M., "Geometric Near-field Characteristics of Supersonic Jets: Full and Laboratory Scales," *Proceedings of Internoise 2012*, 2012, pp. 8082-8092.
- ³⁸Harker, B. M., Gee, K. L., Neilsen, T. B., Wall, A. T., McInerny, S. A., and James, M. M., "Autocorrelation Analysis of Military Jet Aircraft Noise," *Proceedings of Meetings on Acoustics*, Vol. 19, 2013, paper 040072.
- ³⁹Harker, B. M., Gee, K. L., Neilsen, T. B., Wall, A. T., McInerny, S. A., and James, M. M., "On Autocorrelation Analysis of Jet Noise," *Journal of the Acoustical Society of America*, Vol. 133, 2013, pp. EL458 – EL464.
- ⁴⁰Stout, T. A. , Gee, K. L., Neilsen, T. B., Wall, A. T., Krueger, D. W., and James, M. M., "Preliminary Analysis of Acoustic Intensity in a Military Jet Noise Field," *Proceedings of Meetings on Acoustics*, Vol. 19, 2013, paper 040074.
- ⁴¹Morgan, J., Neilsen, T. B., Gee, K. L., Wall, A. T., and James, M. M., "Simple-source Model of High-power Jet Aircraft Noise," *Noise Control Engineering Journal*, Vol. 60, 2012, pp. 435-449.
- ⁴²Hart, D. M., Neilsen, T. B., Gee, K. L. and James, M. M., "A Bayesian-based Equivalent Sound Source Model for a Military Jet Aircraft," *Proceedings of Meetings on Acoustics*, Vol. 19, 2013, paper 055094.
- ⁴³Schlinker, R. H., Simonich, J. C., Shannon, D. W., Reba, R. A., Colonius, T., Gudmundsson, K. and Ladeinde, F., "Supersonic Jet noise from Round and Chevron Nozzles: Experimental Studies," AIAA Paper No. 2009-3257.
- ⁴⁴Gurbatov, S. N. and Rudenko, O. V., "Statistical Phenomena," Chap. 13 in *Nonlinear Acoustics*, edited by M. F. Hamilton and D. T. Blackstock (Academic Press, San Diego, 1998).